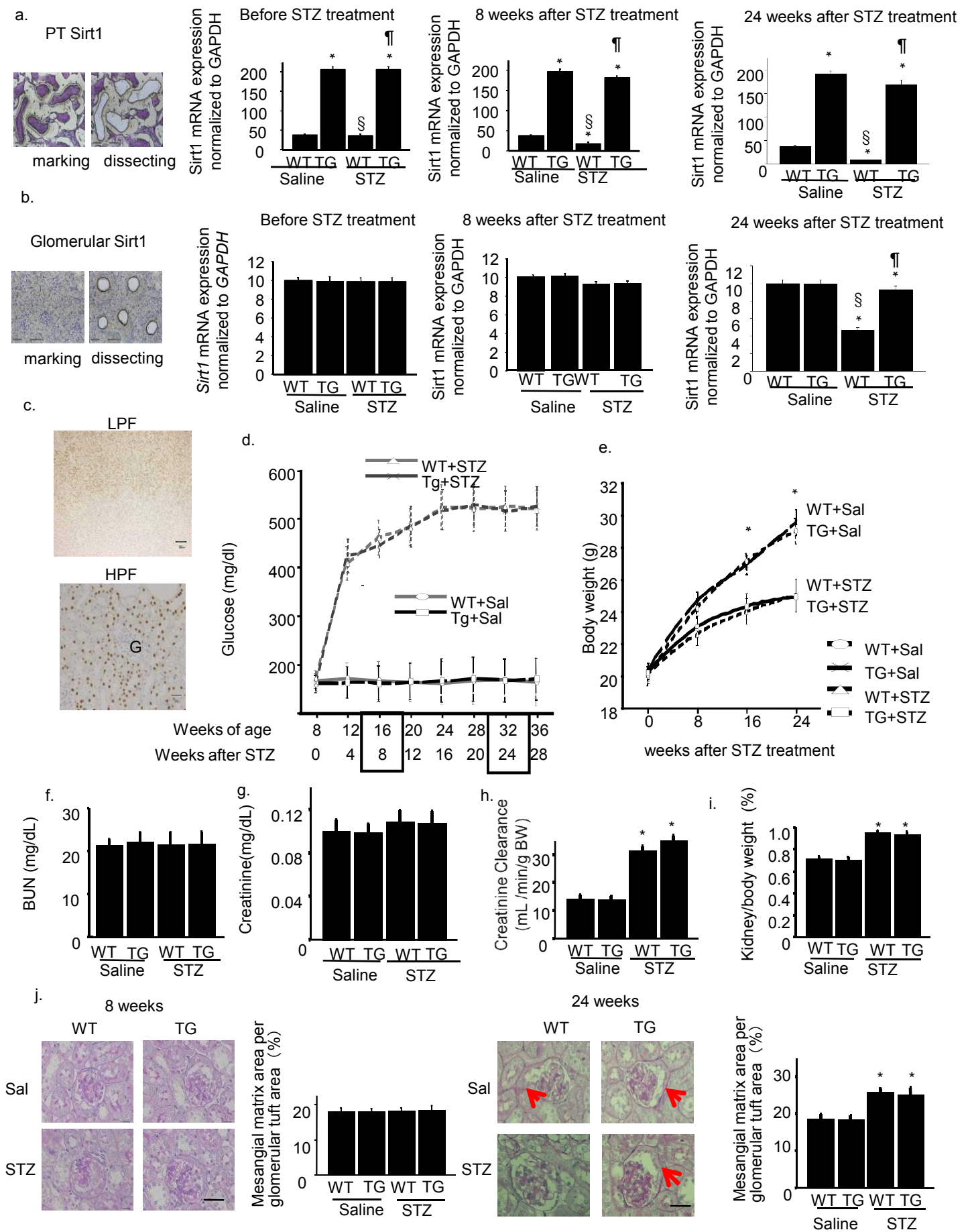


## Supplementary Information

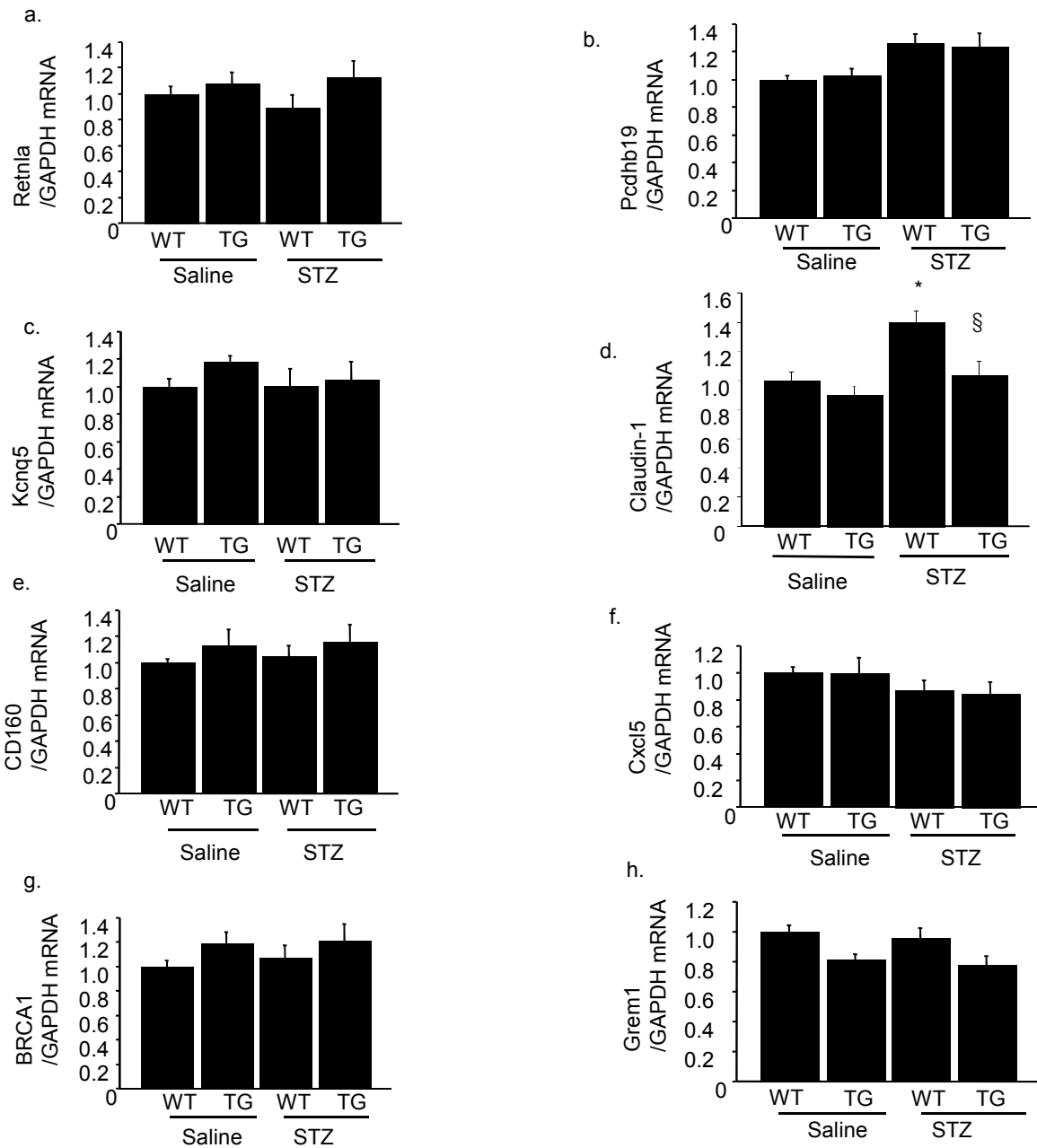
**Journal:** Nature Medicine

<b>Article Title:</b>	<b>Renal tubular Sirt1 attenuates diabetic albuminuria by epigenetically suppressing Claudin-1 overexpression in podocytes.</b>
<b>Corresponding Author:</b>	Shu Wakino

<b>Supplementary Item &amp; Number</b>	<b>Title</b>
Supplementary Figure 1	Phenotypes of proximal tubule-specific <i>Sirt1</i> transgenic mice.
2	Expression of genes of specific interest identified by GeneChip in whole kidneys of proximal tubule-specific <i>Sirt1</i> transgenic mice after STZ treatment.
3	Immunogold electron micrographs for Claudin-1.
4	Expression of Sirt1 and Claudin-1 in proximal tubule-specific <i>Sirt1</i> -deficient mice after STZ treatment and phenotypes of proximal tubule-specific <i>Sirt1</i> transgenic <i>db/db</i> mice.
5	The epigenetic regulation of the <i>Claudin-1</i> gene in HRE cells and in the kidneys of mice with streptozotocin-induced diabetes.
6	Conditioned medium experiment from HK-2 cells cultured in high mannitol medium and NMN levels in proximal tubule-specific <i>Sirt1</i> -deficient mice (CKO).
7	Effects of inhibition of iNampt in mice with streptozotocin-induced diabetes.
8	Schema depicting the retrograde interplay mediated by NMN.
Supplementary Figure Legends	
Supplementary Results	Effects of osmotic changes owing to high glucose medium in CM experiments
Supplementary Table 1	Genes that were up-regulated in the kidneys of TG+STZ mice compared with WT+STZ mice.
2	Genes that were down-regulated in the kidneys of TG+STZ mice compared with WT+STZ mice
3	Clinical data of patients with diabetes and normal controls
4	Sequences used for real-time PCR
5	Primer sequences used for real-time PCR
6	Primer sequences used for methylation-specific PCR

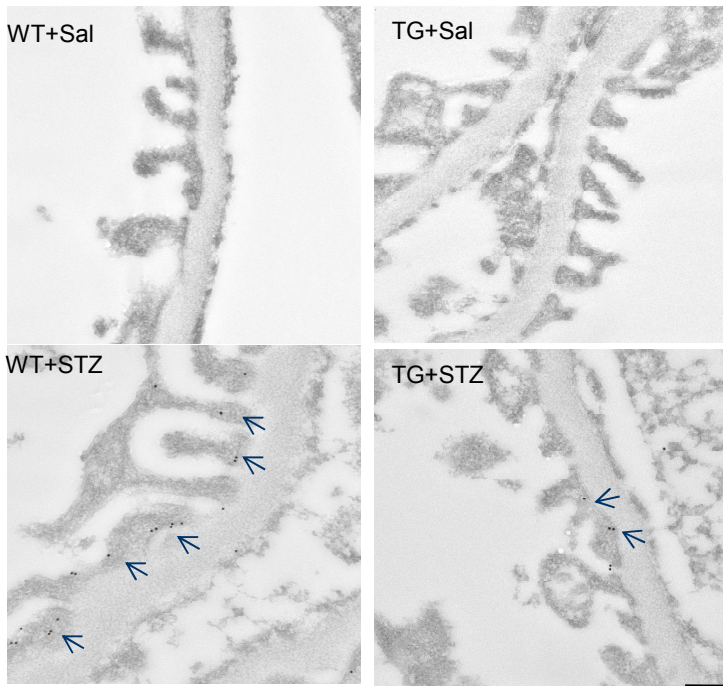


Supplementary Fig. 1, Hasegawa et al.

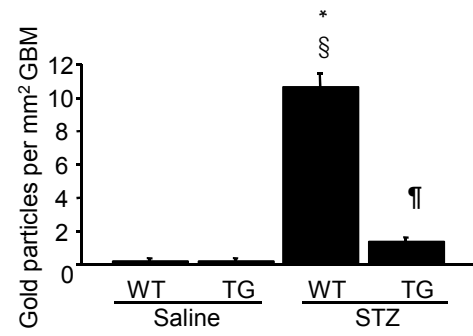


Supplementary Fig. 2, Hasegawa et al.

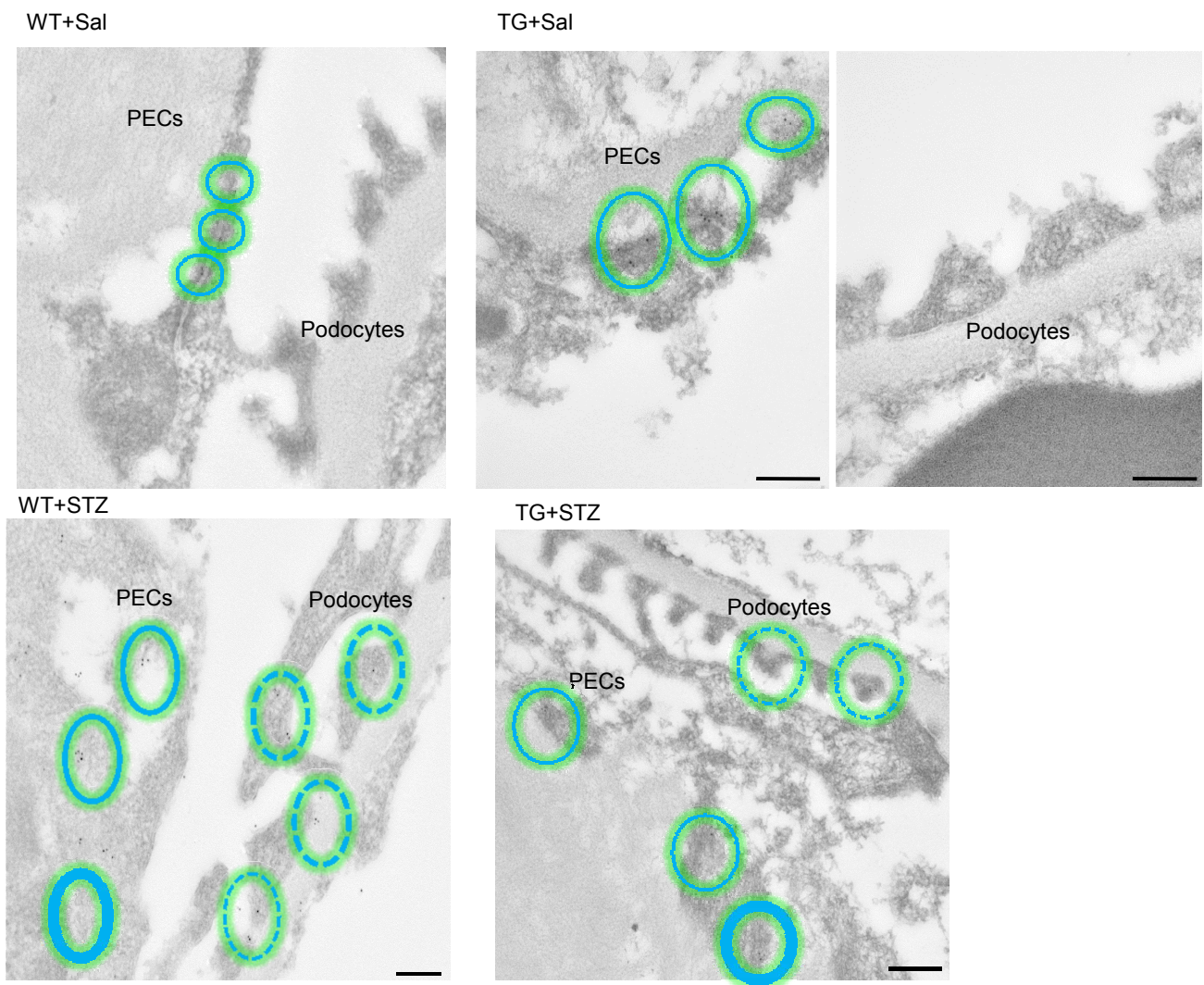
a.

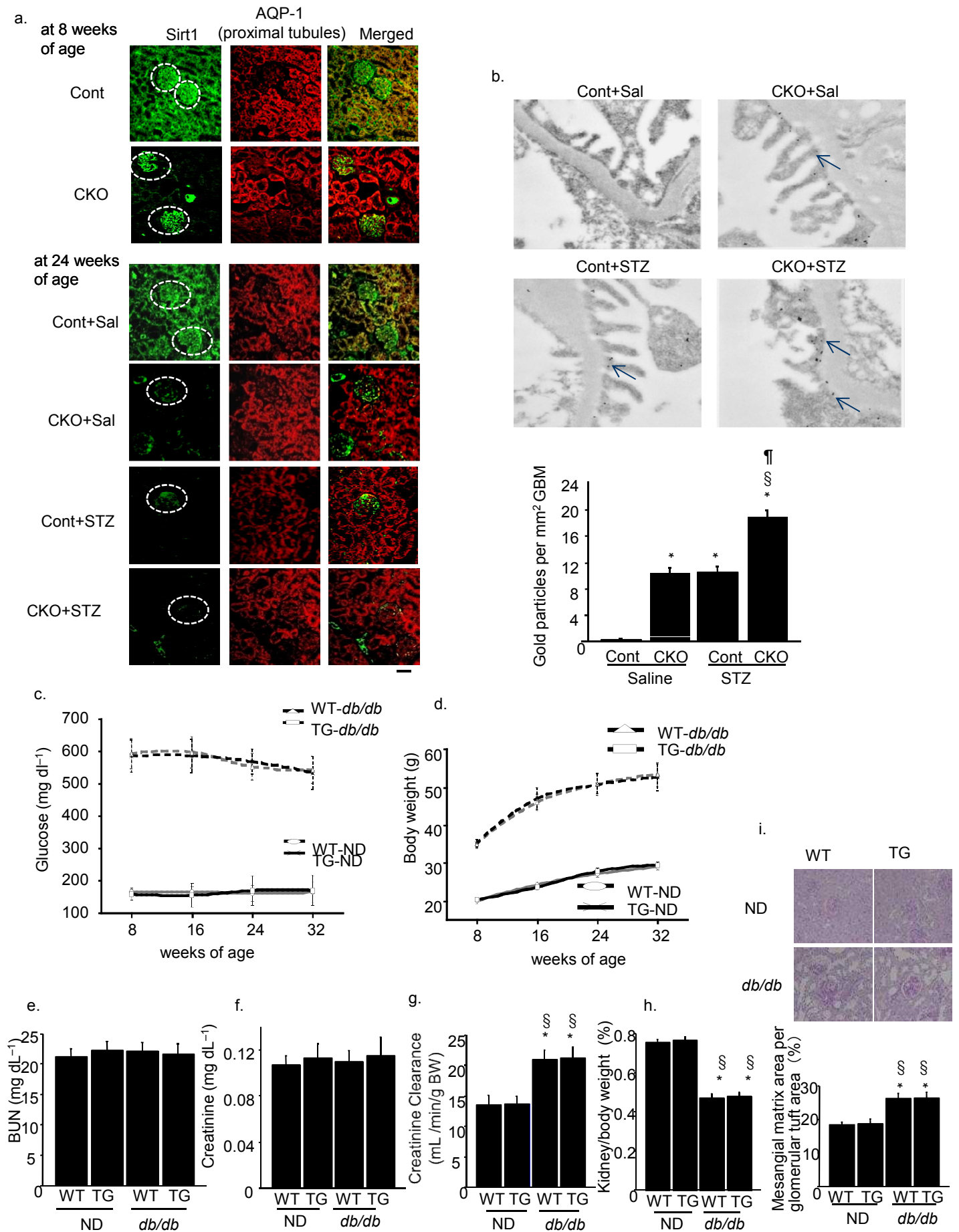


b.

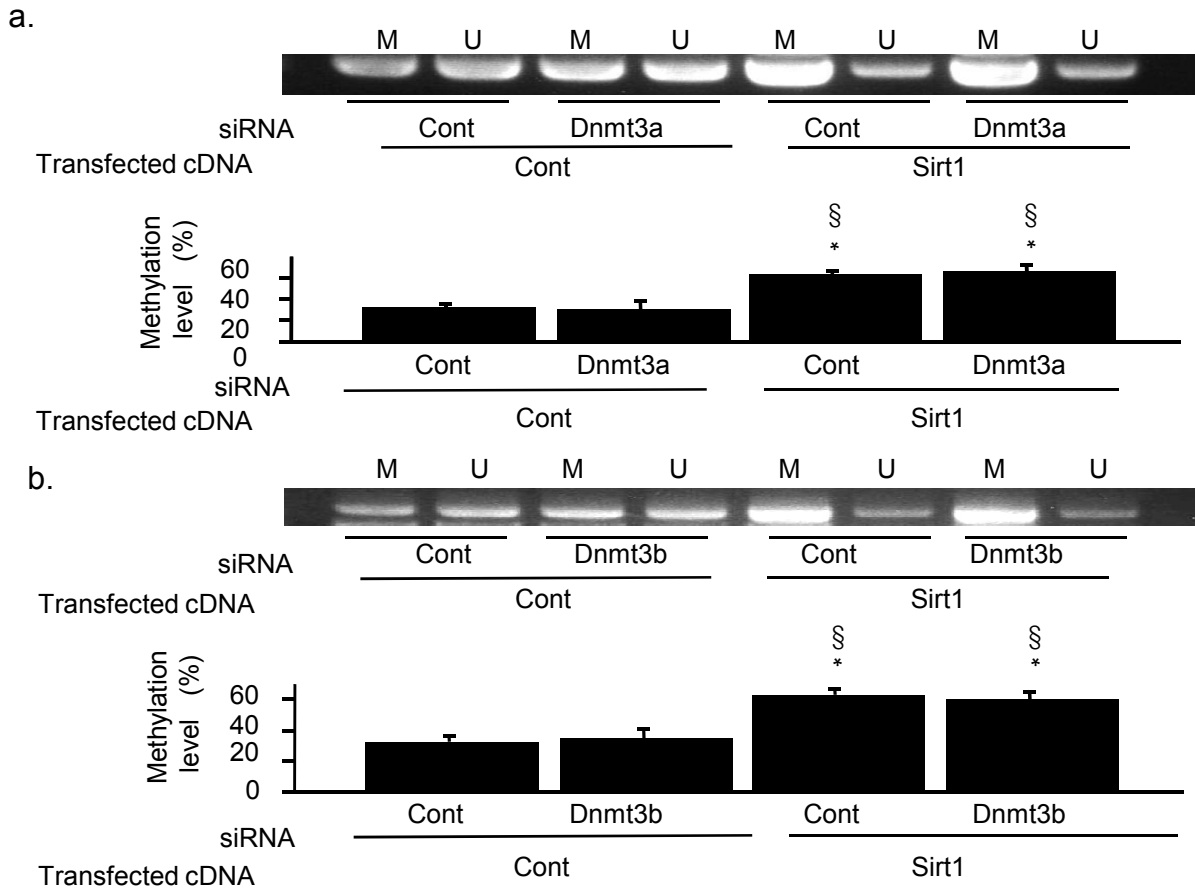


c.





Supplementary Fig. 4, Hasegawa et al.

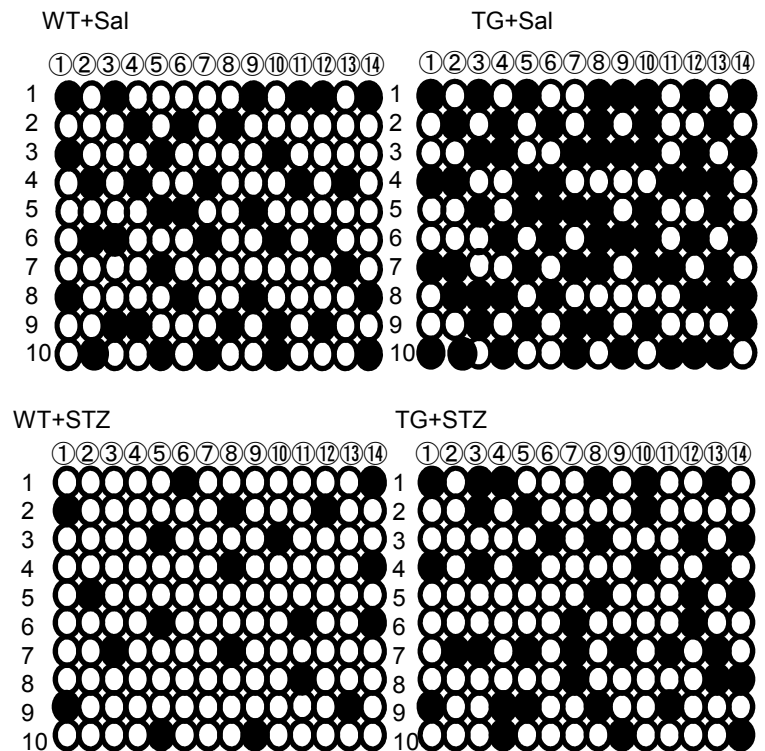


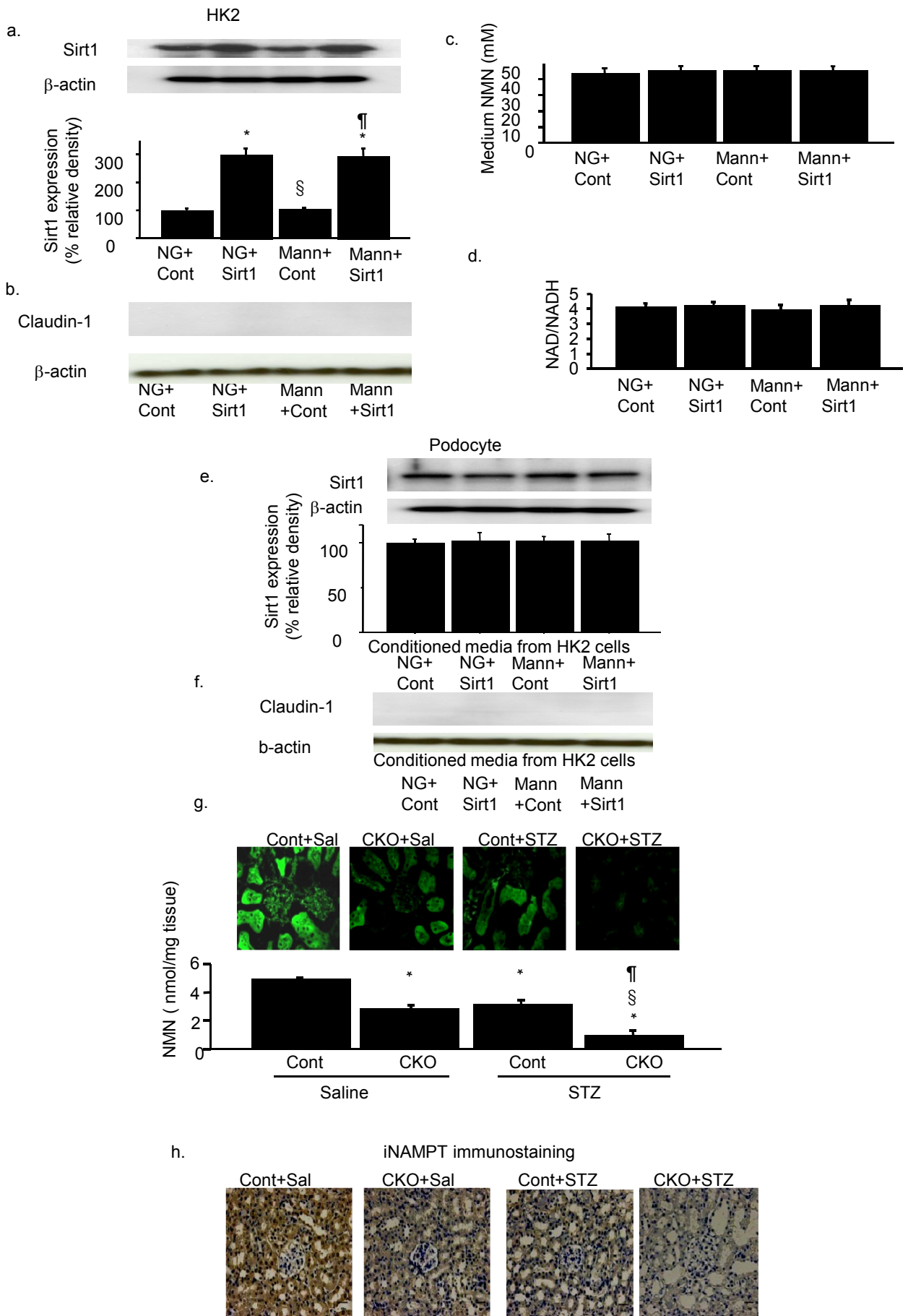
**c.**

ccagaagccaggagcct cgccccgcagctgcacagagagcaagggtata  
ggcactaactgtttgcagagaccccatcaccttcgggagctcaggtgcga  
①② ③  
ccttgaactccactttctgcatctgccactgagcccgcgaggagcctcggaa  
start codon ④⑤  
agagccatggccaaacgcggggctgcagctgctgggtttcatcctgcttct  
⑥ ⑦  
gggatgatcggtccatcgtcagcactgccctgcccagtggaagattact  
⑧ ⑨ ⑩  
cctatgctggggacaacatcgtgaccgctcaggccatctacgagggactgtg  
⑪ ⑫ ⑬ ⑭  
gatgtcctgcgttcgcaaagcaacgggcagatacagtgcaaagtctcgact

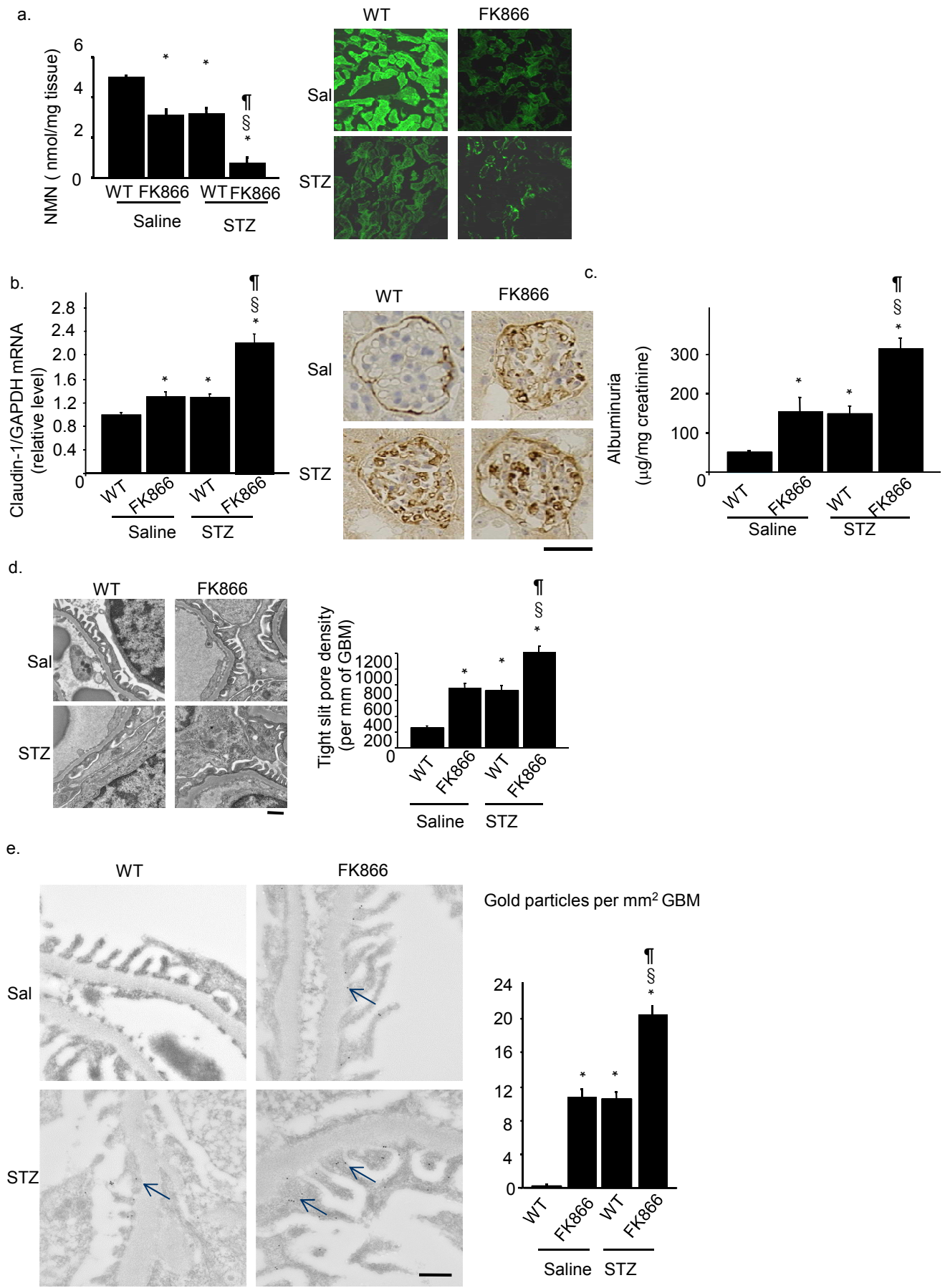
ccttctggaatctgaacagctactttgcaggcaaccggagccttgatggtaattg  
gcatcctgctggggctgacgcaatctttgtgtccaccattggcatgaagtcat

**d.**

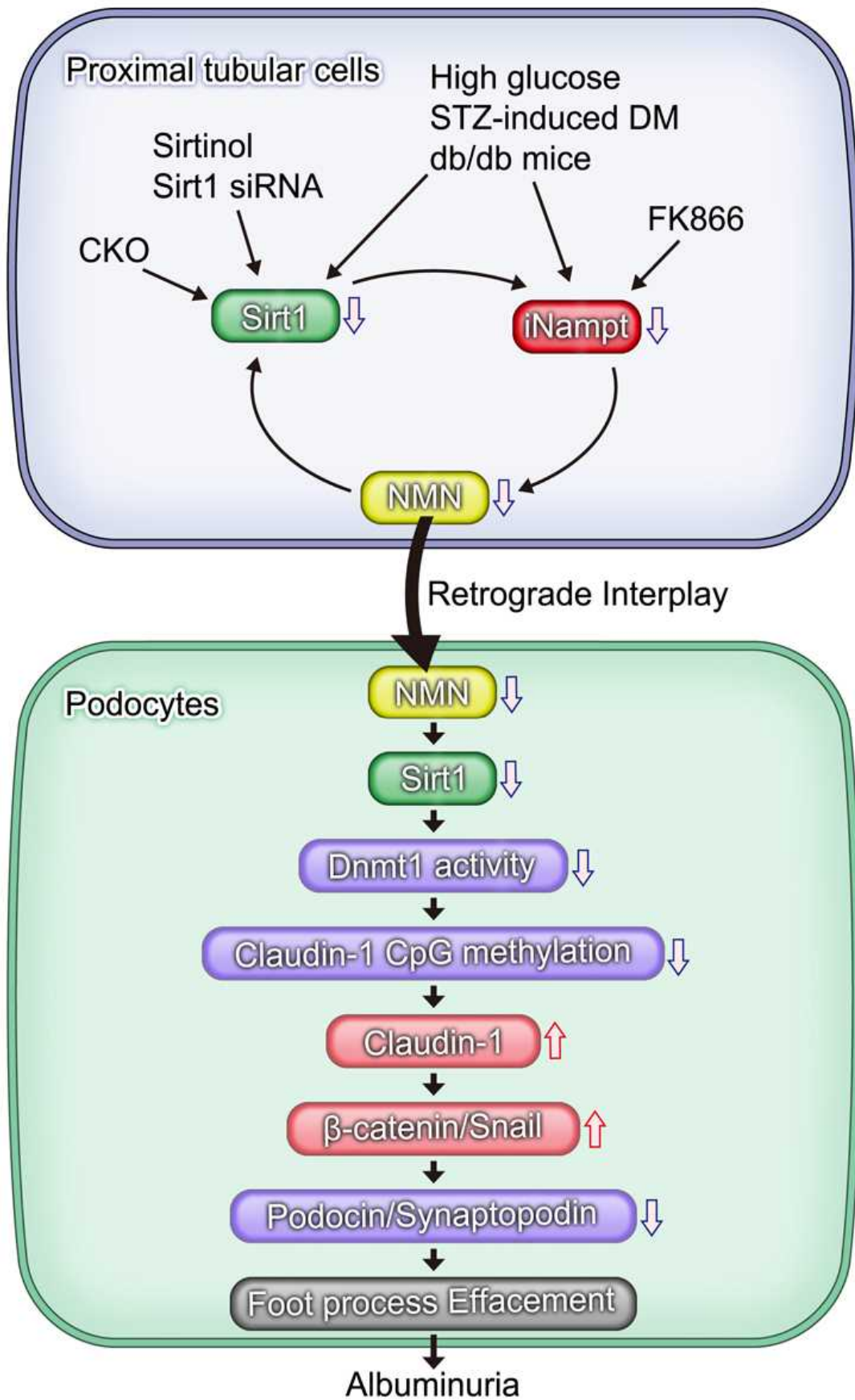




Supplementary Fig. 6, Hasegawa et al.



Supplementary Fig. 7, Hasegawa et al.



Supplementary Fig. 8, Hasegawa et al.

## Supplementary Figure Legends

**Supplementary Figure 1** Phenotypes of proximal tubule-specific *Sirt1* transgenic mice. **(a, b)** Renal cell-specific changes in *Sirt1* **(a)** and *Claudin-1* **(b)** mRNA expression in proximal tubule-specific *Sirt1* transgenic mice (TG) and wild-type mice (WT). We successfully marked and dissected different nephron segments including proximal tubular (PT) cells and glomeruli. The levels of mRNAs for *Sirt1* and *Claudin-1* were measured by real-time PCR in TG and WT mice before, 8 weeks and 24 weeks after streptozotocin (STZ) or saline (Sal) treatment. \* $P < 0.05$  vs. WT+Sal, § $P < 0.05$  vs. TG+Sal, ¶ $P < 0.05$  vs. WT+STZ,  $n = 8$ . **(c)** Predominant *Sirt1* expression in proximal tubules in the kidneys of TG mice assessed by immunostaining for FLAG. Scale bars, 500  $\mu\text{m}$  (upper panel; low power field, LPF,  $\times 100$ ) and 100  $\mu\text{m}$  (lower panel; high power field, HPF,  $\times 400$ ). **(d)** Temporal changes in mean plasma glucose concentrations in mice in each group. We sacrificed the mice 8 weeks and 24 weeks after treatment, corresponding to 16 and 32 weeks of age (black boxes). **(e)** Body weight changes from 0 to 24 weeks after STZ or Sal treatment in WT or TG mice. Plasma BUN **(f)** and plasma creatinine **(g)** concentrations, creatinine clearance **(h)** and the ratio of kidney weight to body weight **(i)** of mice in each experimental group. **(j)** Representative PAS staining 8 weeks (left) and 24 weeks (right) after STZ treatment. The bar graph shows the quantification of mesangial matrix deposition indicated as the ratio to glomerular tuft area. Scale bar, 50  $\mu\text{m}$ . \*\*  $P < 0.01$  vs. WT+Sal, \*  $P < 0.05$  vs. WT+Sal.  $n = 8$ .

**Supplementary Figure 2** Expression of genes of specific interest identified by GeneChip in whole kidneys of proximal tubule-specific *Sirt1* transgenic mice after STZ treatment. Changes in expression of the genes identified by GeneChip were examined using whole kidney samples and real-time PCR. Expression of *Retnla* **(a)**, *Pcdh19* **(b)**, *Kcnq5* **(c)**, *Claudin-1* **(d)**, *CD160* **(e)**, *Cxcl5* **(f)**, *BRCA1* **(g)**, and *Grem1* **(h)** in whole kidney.  $n = 8$ .

**Supplementary Figure 3** Immunogold electron micrographs for Claudin-1. **(a)** Representative

immunogold electron micrographs for Claudin-1 in the kidney of proximal tubule-specific *Sirt1* transgenic mice (TG) or wild-type mice (WT) after streptozotocin (STZ) or saline (Sal) treatment. Arrows indicate immunogold particles. Scale bar, 0.5  $\mu\text{m}$ . **(b)** Numbers of gold particles  $\mu\text{m}^{-2}$  glomerular basement membrane (GBM). \* $P < 0.05$  vs. WT+Sal, § $P < 0.05$  vs. TG+Sal, ¶ $P < 0.05$  vs. WT+STZ,  $n = 8$ . **(c)** Representative immunogold electron micrographs for Claudin-1 for each group of mice. Claudin-1 expression was detectable in PECs and was undetectable in podocytes in non-diabetic, WT+Sal or TG+Sal mice. Higher levels of Claudin-1 were seen in the PECs and podocytes of WT+STZ mice compared with WT+Sal mice, but lower levels were seen in these regions in TG+STZ mice compared with TG+Sal mice. Blue ovals indicate immunogold particles. Scale bar, 0.5  $\mu\text{m}$ .

**Supplementary Figure 4** Expression of *Sirt1* and Claudin-1 in proximal tubule-specific *Sirt1*-deficient mice after STZ treatment and phenotypes of proximal tubule-specific *Sirt1* transgenic *db/db* mice. **(a)** Kidney cryosections derived from proximal tubule (PT)-specific *Sirt1*-deficient mice (CKO) or control mice (cont) treated with streptozotocin (STZ) or saline (Sal) were subjected to fluorescence immunohistochemistry staining for *Sirt1* (green color) by applying the monoclonal anti-*Sirt1* antibody and staining with anti-AQP1 (red color), a PT marker. White dotted lines highlight glomeruli. Scale bar, 20  $\mu\text{m}$ . Upper panel; Cont and CKO mice at 8 weeks of age. Lower panel; Cont+Sal, CKO+Sal, CKO+Sal, and CKO+STZ mice at 24 weeks after treatment (e.g., at 32 weeks of age). **(b)** Representative immunogold electron micrographs for Claudin-1. Arrows indicate immunogold particles for Claudin-1 protein. Scale bar, 0.5  $\mu\text{m}$ . The bar graph shows the numbers of gold particles  $\mu\text{m}^{-2}$  glomerular basement membrane (GBM). \* $P < 0.05$  vs. Cont+Sal, § $P < 0.05$  vs. CKO+Sal, ¶ $P < 0.05$  vs. Cont+STZ,  $n = 8$ . **(c-i)** We crossed our proximal tubule-specific *Sirt1* transgenic mice (TG) with obese *db/db* mice (*db/db*). Fasting blood glucose levels **(c)** and body weight **(d)** in WT-*db/db* and TG-*db/db* mice as compared with those in nondiabetic mice (WT-ND and TG-ND). Plasma BUN **(e)** and plasma creatinine **(f)** concentrations,

creatinine clearance (**g**) and the ratio of kidney weight to body weight (**h**) in each group of mice. \* $P < 0.05$  vs. WT-ND, § $P < 0.05$  vs. TG-ND,  $n = 8$ . (i) Representative PAS staining of kidney in mice at 32 weeks of age. The bar graph lower panel shows the quantification of mesangial matrix deposition indicated as the ratio to glomerular tuft area. Scale bar; 50  $\mu\text{m}$ . \*  $P < 0.05$  vs. WT-ND, §  $P < 0.05$  vs. TG-ND.  $n = 8$ .

**Supplementary Figure 5** The epigenetic regulation of the *Claudin-1* gene in HRE cells and in the kidneys of mice with streptozotocin-induced diabetes. (a,b) The involvement of Dnmt in Sirt1-mediated *Claudin-1* gene methylation. Methylation of the *Claudin-1* gene was examined with or without the transfection of *Sirt1* expression vectors. SiRNA for *Dnmt3a* (a) or *Dnmt3b* (b) was co-transfected. The bar graph shows the results of densitometry analysis. \* $p < 0.05$  vs. control cDNA and control siRNA-transfected cells, § $p < 0.05$  vs. control cDNA and *Dnmt* siRNA-transfected cells,  $n = 5$ . M indicates methylated DNA, and U indicates unmethylated DNA. (c) CpG islands on the *Claudin-1* gene. Each number indicates the position of a CpG island. (d) Bisulfite genomic sequencing (BGS) of the micro-dissected PECs in proximal tubule-specific *Sirt1* transgenic mice (TG) with STZ or saline (Sal) treatment. Each box is representative of the indicated mouse group; each row of dots in the boxes is representative of the *Claudin-1* CpG island; each dot is representative of a single CpG. Empty dots indicate unmethylated CpGs; black dots indicate methylated CpGs. Each row represents a single sequenced clone (ten for each group of mice).

**Supplementary Figure 6** Conditioned medium experiment from HK-2 cells cultured in high mannitol medium and NMN levels in proximal tubule-specific *Sirt1*-deficient mice (CKO). (a-f) HK-2 cells were cultured under the four conditions of NG (normal glucose)+Cont (control vector), NG+Sirt1 (*Sirt1* expression vector), Mann (high mannitol)+Cont and Mann+Sirt1. (a) Immunoblotting for *Sirt1* (upper panel) and densitometry analysis of the results (lower panel). (b) Immunoblotting for *Claudin-1*. (c,d) NMN levels (c) and NAD/NADH ratio (d) of each conditioned

medium from HK-2 cells. **(e,f)** Podocytes were cultured in the conditioned media from these HK-2 cells. Sirt1 expression **(e)** and Claudin-1 expression **(f)** in podocytes were examined. \* $P < 0.05$  vs. NG+Cont, § $P < 0.05$  vs. NG+Sirt1, ¶ $P < 0.05$  vs. Mann+Cont,  $n = 5$ . **(g, h)** Tissue NMN levels **(g)** and iNAMPT immunostaining **(h)** among four groups of mice (Cont+Sal, CKO+Sal, Cont-STZ and CKO+STZ). \*  $P < 0.05$  vs. Cont+Sal, ¶ $P < 0.05$  vs. Cont+STZ,  $n = 5$ .

**Supplementary Figure 7** Effects of inhibition of iNampt in mice with streptozotocin-induced diabetes. **(a)** Tissue NMN levels among four groups of mice (WT+Sal, FK866+Sal, WT+STZ and FK866+STZ).  $n = 5$ . Representative intracellular autofluorescence images of NMN in the kidney of each group of mice are shown in the right panel. **(b)** Immunostaining for Claudin-1 in kidneys from each experimental group. The left panel shows mRNA expression for *Claudin-1*. Scale bar, 50  $\mu\text{m}$ . **(c)** Albuminuria of mice in each experimental group.  $n = 8$ . **(d)** Electron photomicrographs (30,000  $\times$  magnification) of the kidneys of mice in each experimental group. The bar graph shows the tight slit pore densities. Scale bar, 500 nm. **(e)** Representative immunogold electron micrographs for Claudin-1. Arrows indicate immunogold particles for Claudin-1 molecules. Scale bar, 0.5  $\mu\text{m}$ . The bar graph shows the numbers of gold particles  $\mu\text{m}^{-2}$  glomerular basement membrane (GBM). **(a-e)** \* $P < 0.05$  vs. WT+Sal, § $P < 0.05$  vs. FK866+Sal, ¶ $P < 0.05$  vs. WT+STZ,  $n = 5$ .

**Supplementary Figure 8** Schema depicting the retrograde interplay mediated by NMN. The downregulation of Sirt1 or iNAMPT by various conditions leads to NMN deficiency in proximal cells, which propagates to PECs or podocytes. The lower level of NMN in podocytes causes the downregulation of Sirt1, which upregulates Claudin-1 expression and leads to albuminuria.

## **Supplementary Results**

### **Effects of osmotic changes owing to high glucose medium in CM experiments**

To rule out the possibility of an osmotic effect induced by high glucose medium, experiments were also performed using mannitol (5 mM glucose+15 mM mannitol, Mann), which has the same osmotic pressure as HG (25 mM glucose). Immunoblotting showed that Sirt1 cDNA transfection induced an approximately 3-fold higher Sirt1 protein level in the NG+Sirt1 condition compared with the NG+Cont condition. Sirt1 expression was not reduced in the Mann+Cont condition (**Supplementary Fig. 6a**). Immunoblotting revealed an absence of Claudin-1 protein expression in all four groups of HK2 cells (**Supplementary Fig. 6b**). The medium NMN and intracellular NAD/NADH concentrations were similar in the NG+Cont, NG+Sirt1, Mann+Cont and Mann+Sirt1 conditions (**Supplementary Fig. 6c,d**). Exposure to the media collected from NG+Cont and NG+Sirt1 cells did not influence the podocytes. Moreover, the medium from Mann+Cont cells did not reduce the levels of Sirt1 and Claudin-1 in podocytes (**Supplementary Fig. 6e and 6f**). These data negated the possibility of osmotic effects induced by the high glucose medium.

**Supplementary Table 1. Genes that were up-regulated in the kidneys of TG+STZ mice compared with WT+STZ mice**

<b>Gene Symbol</b>	<b>Gene Name</b>	<b>Fold Change</b>	<b>Genbank Accession</b>
Gm5494	predicted gene 5494	23.423	NM_001177529
Gm14137	predicted gene 14137	22.333	NM_001039223
Adipoq	adiponectin, C1Q and collagen domain containing	20.799	NM_009605
Gm1330	predicted gene 1330	19.591	XM_485073
Retnla	resistin like alpha	17.670	NM_020509
Popdc3	popeye domain containing 3	16.303	NM_024286
Gm12836	cytochrome P450, family 4, subfamily a, polypeptide 30a, pseudogene	14.960	XM_621635
LOC634100	similar to Ig heavy chain V region 108A precursor	14.420	
Kcnq5	potassium voltage-gated channel, subfamily Q, member 5	13.217	NM_023872
LOC100046894	similar to Igk-C protein	12.193	XM_001477017
H60a	histocompatibility 60a	12.001	NM_010400
Mmp21	matrix metalloproteinase 21	11.882	NM_152944
Cd160	CD160 antigen	11.234	NM_018767
LOC639930	similar to Ig heavy chain V-I region HG3 precursor	10.940	U58290
Brcal	breast cancer 1	10.818	NM_009764
1700049L16Rik	hematological and neurological expressed 1-like pseudogene	10.707	NR_003644
H60b	histocompatibility 60b	10.498	NM_001177775
LOC677643	similar to Ig heavy chain V region 3 precursor	10.295	XR_031047
LOC100046827	similar to CG13990-PA	9.735	XM_001476858
Gm1409	predicted gene 1409	9.545	XM_357633
Olf118	olfactory receptor 118	9.391	NM_213721
Fbxw26	F-box and WD-40 domain protein 26	9.383	NM_198674
Gm4439	predicted gene 4439	9.001	XM_001480174
Vmn2r120	vomer nasal 2, receptor 120	8.874	NM_001104591
Adcy10	adenylate cyclase 10	8.432	NM_173029

**Supplementary Table 2. Genes that were down-regulated in the kidneys of TG+STZ mice compared with WT+STZ mice**

<b>Gene Symbol</b>	<b>Gene Name</b>	<b>Fold Change</b>	<b>Genbank Accession</b>
2410017I17Rik	RIKEN cDNA 2410017I17 gene	0.040	AK082845
Sycp1	synaptonemal complex protein 1	0.046	NM_011516
Zfp541	zinc finger protein 541	0.060	NM_001099277
Pcdhb19	protocadherin beta 19	0.060	NM_053144
LOC665788	similar to spermiogenesis specific transcript on the Y 1	0.060	XM_001487820
Try4	trypsin 4	0.065	NM_011646
LOC674135	similar to RT1 class I histocompatibility antigen, AA alpha chain precursor	0.067	XR_004604
1700049E22Rik	RIKEN cDNA 1700049E22 gene	0.071	XM_001479989
4933426D04Rik	RIKEN cDNA 4933426D04 gene	0.073	AK016926
Cldn1	Claudin 1	0.077	NM_016674
Olf463	olfactory receptor 463	0.077	NM_146413
AI415467	expressed sequence AI415467	0.080	EC277811
Gm13011	predicted gene 13011	0.080	NM_001126318
Mro	maestro	0.082	NM_027741
Cxcl5	chemokine (C-X-C motif) ligand 5	0.083	NM_009141
C230055K05Rik	RIKEN cDNA C230055K05 gene	0.083	NM_001039231
Try5	trypsin 5	0.084	NM_001003405
Gm9495	predicted gene 9495	0.086	XM_001475988
Muc19	mucin 19	0.087	NM_207243
Gm11201	predicted gene 11201	0.090	AK154065
Gm5112	predicted gene 5112	0.096	XM_001480114
Slfn1	Schlafen-like 1	0.105	NM_177570
1700018F24Rik	RIKEN cDNA 1700018F24 gene	0.107	NM_027069
Grem1	gremlin 1	0.107	NM_011824
Kif7	kinesin family member 7	0.112	NM_010626
Gm6590	predicted gene 6590	0.113	XM_001480319
LOC100044228	hypothetical protein LOC100044228	0.114	XM_001471920
Gm2931	predicted gene 2931	0.115	XM_001475142
4930422I22Rik	RIKEN cDNA 4930422I22 gene	0.123	AK015180

**Supplementary Table 3. Clinical data of patients with diabetes and normal controls**

<b>Sample name</b>	<b>Gender</b>	<b>Age (years)</b>	<b>Serum creatine (mg/dL)</b>	<b>Proteinuria (g /day)</b>	<b>eGFR (ml/min/1.73m<sup>2</sup>)</b>	<b>HbA1c (%)</b>
<b>Diabetic Nephropathy</b>						
<b>DN-1</b>	<b>male</b>	<b>83</b>	<b>1.81</b>	<b>1.6</b>	<b>28.5</b>	<b>6.6</b>
<b>DN-2</b>	<b>male</b>	<b>42</b>	<b>1.13</b>	<b>4.9</b>	<b>58.1</b>	<b>6.3</b>
<b>DN-3</b>	<b>male</b>	<b>62</b>	<b>1.73</b>	<b>1.5</b>	<b>32.6</b>	<b>6.1</b>
<b>DN-4</b>	<b>male</b>	<b>47</b>	<b>1.82</b>	<b>5.4</b>	<b>33.4</b>	<b>6.1</b>
<b>DN-5</b>	<b>male</b>	<b>80</b>	<b>1.23</b>	<b>10.2</b>	<b>44.0</b>	<b>6.0</b>
<b>DN-6</b>	<b>male</b>	<b>56</b>	<b>2.93</b>	<b>12.0</b>	<b>18.9</b>	<b>6.4</b>
<b>DN-7</b>	<b>male</b>	<b>75</b>	<b>1.57</b>	<b>1.4</b>	<b>33.6</b>	<b>6.1</b>
<b>DN-8</b>	<b>male</b>	<b>59</b>	<b>1.88</b>	<b>0.5</b>	<b>71.2</b>	<b>5.8</b>
<b>DN-9</b>	<b>female</b>	<b>64</b>	<b>1.89</b>	<b>2.9</b>	<b>36.3</b>	<b>6.1</b>
<b>DN-10</b>	<b>female</b>	<b>51</b>	<b>0.54</b>	<b>4.6</b>	<b>91.0</b>	<b>5.9</b>
<b>DN-11</b>	<b>male</b>	<b>61</b>	<b>0.69</b>	<b>7.7</b>	<b>89.0</b>	<b>7.2</b>
<b>Controls</b>						
<b>CO-1</b>	<b>female</b>	<b>39</b>	<b>0.61</b>	<b>&lt;0.1</b>	<b>86.2</b>	<b>5.2</b>
<b>CO-2</b>	<b>male</b>	<b>27</b>	<b>0.87</b>	<b>&lt;0.1</b>	<b>88.1</b>	<b>4.9</b>
<b>CO-3</b>	<b>female</b>	<b>51</b>	<b>0.64</b>	<b>&lt;0.1</b>	<b>76.7</b>	<b>5.3</b>
<b>CO-4</b>	<b>female</b>	<b>35</b>	<b>0.66</b>	<b>&lt;0.1</b>	<b>84.9</b>	<b>5.0</b>
<b>CO-5</b>	<b>male</b>	<b>42</b>	<b>0.83</b>	<b>&lt;0.1</b>	<b>81.4</b>	<b>5.5</b>

Clinical parameters in patients with diabetic nephropathy (DN) at the time of needle renal biopsy or in living donors (CO; normal kidneys) at the time of pre-transplant biopsies.

**Supplementary Table 4. Sequences used for real-time PCR**

Gene	Sequences (5'-3')		Accession
	Forward	Reverse	
GAPDH	CATCAGTCCTTCCACGATACCA	CCTGCACCACCAACTGCTTA	NM_008084.2
Retnla	TTGCCTGTGGATCTTGGGAG	TTCTCCCTATGTTTCCTAACC	NM_020509.3
Kcnq5	GGGCACAATCACACTGACAACC	GAAAGAAATGCCAAGGAGTGCG	NM_023872.3
CD160	TGCAGGATGCTGTTGGAACCC-	CCTGTGCCCTGTTGCATTCTTG	NM_018767.3
BRCA1	CCGGATACGAGAGTGAAACAA	TGCTGCAGCTTTATCAGGTT	NM_008676.3
Pcdhb19	TTTAGGAGAAACTACCTTGTGC	TGAGCATTAAAGTCACTTGAGG	NM_053144.2
Claudin-1	CCCAGTGGAAGATTACTCCTAGT	TGCAAAGTACTGTTTCAGATTCAGC	NM_016674.4
Cxcl5	CAT CGC CAG CGC TGG TCC T	GGG ATG AAC TCC TTG CGT GGT CT	NM_009141.2
Grem1	GCAAAACCCAGCCGCTTAA	TGATGGTGCGACTGTTGCA	NM_011824.4

**Supplementary Table 5. Primer sequences used for real-time PCR**

Gene	Sequences (5'-3')		Accession
	Forward	Reverse	
GAPDH	CATCAGTCCTTCCACGATACCA	CCTGCACCACCAACTGCTTA	NM_008084.2
Claudin-1	CCCAGTGGAAGATTTACTCCTAGT	TGCAAAGTACTGTTTCAGATTCAGC	NM_016674.4
Dnmt1	AGTGCAAGGCGTGCAAAGATATGG	TGGGTGATGGCATCTCTGACACAT	NM_010066.3
Sirt1	GATCCTTCAGTGTCATGGTT	GAAGACAATCTCTGGCTTCA	NM_019812
$\beta$ -catenin	TCAGAGGGTCCGAGCTGCCA	TGTCAGCTCAGGAATTGCAC	NM_001081088
Snail	GAGGCGGTGGCAGACTAG	GACACATCGGTCAGACCAG	NM_011040
Synptopodin	TGGACTGGTGGACATTGAAA	TTACAACGGTCTGTGGTGA	NM_019459.2
Podocin	GTGTCCAAAGCCATCCAGTT	GACCTTCCTTCTCGTAACG	NM_001163574.1

**Supplementary Table 6. Primer sequences used for methylation-specific PCR**

Primer set	Primer sequence (5'→3')	Product size	Sequence number	Annealing temperature
Human Claudin-1-M methylated primers	Forward: GTTGTAGTTGTTGGGTTTTATTTTC Reverse: AACCTAAACGATCACGATATTATCG	121	255–279 375–399	65°C
Human Claudin-1-U unmethylated primers	Forward: GGTTGTAGTTGTTGGGTTTTATTTTT Reverse: TACATAACCTAAACAATCACAATATTATC	127	254–279 380–409	65°C

